The First Pan American Geosynthetics Conference & Exhibition
2-5 March 2008, Cancun, Mexico

Behavior of Geogrids under Different Strain Level

Huai-Houh Hsu, Department of Civil Engineering, Chienkuo Technology University, Changhua, Taiwan
Yu-Hsien Ho, Technical Support Dep., ACE Geosynthetic Enterprise Co.,Ltd., Taichung, Taiwan

ABSTRACT
To get a well prediction of working stress analysis, the decision of material properties is important. A series of monotonic tensile loading tests are carried out to demonstrate PET geogrids' behavior under three strain levels (1%, 3%, and 4.5%). The small range of load-strain curve (i.e. local strain less than 0.3%) at each strain level is established by a new developed measurement system. This system is mainly composed of a stepper motor, a load cell, two linear variable differential transducers, two non-contact proximitors, and a 22 bits analog/digital converter. The test results show that the new system can get a clear trend of local load-strain curve at each strain level to provide a well estimation of stiffness.

RESUMEN
Para obtener un buen resultado de las predicciones del análisis de tensión, es importante las propiedades y el material a utilizar. La prueba monotonica de carga de tensión ha logrado demostrar que los geogrid (PET) funciona bajo tres niveles de tensión (1%, 3% y 4.5%). En la curva aparecen pequeños puntos de carga de tensión (i.e. estos son menos de 0.3%), por lo cual se diseño un nuevo sistema de medida para estos niveles. Este sistema esta principalmente compuesto por niveles de rotación del motor; sensor de carga; dos líneas diferenciales del transductor; y un convertidor análogo/digital de 22 bits. El resultado del nuevo sistema muestra una tendencia en la carga de la tensión local, dando como resultado una buena estimación de la rigidez.

1. INTRODUCTION

Geogrid material is widely used in geotechnical engineering field to construct soil reinforced structures. The Mechanically Stabilized Earth Wall (MSEW) is one of the popular earth retaining structures for slope stability. The safety of MSEW is generally determined by limited equilibrium analysis (LEA). This method can obtain a safety factor at an assumed failure surface but can not provide the stress and strain states of MSEW. This will cause a conservative but less economic design. Allen and Bathurst (2002) collected in situ data of 16 full size MSEW and found out the deformation was smaller than the prediction value of LEA. Working stress analysis (WSA) has been developed and attempts to solve this problem. By means of finite element or finite difference methods, WSA can predict the distribution of stress and strain of MSEW at different construction stages as well as operation period. Allen and Bathurst (2003) adopted the frame of WSA to develop the K-stiffness method. A batch of monitoring data obtained from 54 full-scale MSEWs were compared with predict values of K-stiffness method. Results show that K-stiffness method can raise economical profit of constructing MSEW efficiently.

To obtain well prediction values by WSA, the decision of material strength parameters are important. Atkison and Sallfors (1991) divided soil strain into three stages:
(1) very small strain: shear strain is smaller than 1×10^{-3}%
(2) small strain: shear strain is between 1×10^{-3}% and 1%
(3) large strain: shear strain is greater than 1%

The shear strain of a retaining wall is between 0.01% and 0.1% (Atkinson, 2000). In most cases of MSEW, the peak strain is no more than 2% at the end of construction (Bathurst et al., 2002). The dynamic soil properties can be obtained from dynamic or cyclic laboratory tests. The material properties of geogrid should be known in a small strain range at different strain levels as well. Factors that affect geosynthetic stiffness include (Walters et al., 2002):
(1) loading sequence
(2) rate of loading and time
(3) confining pressure of soil
(4) strain level
(5) temperature
(6) installation damage

Bathurst and Cai (1994) carried out a series of cyclic load-extension tests to investigate the performance of HDPE and PET geogrids. When the strain was greater than 2% and loading frequency was higher than 0.5 Hz, the stiffness of cyclic unload-reload curve of HDPE decreased with increasing strain. The cyclic unload-reload stiffness of PET increased when strain level is higher than 3%. The stiffness at different strain level could be varied due to its loading history. For

reasonably predicting the behavior of MSEW by WSA, the material properties of geogrids should be obtained in a small strain range at different strain levels.

2. SMALL STRAIN MEASUREMENT SYSTEM

In order to establish the global load – strain curve and local strain curve at different strain level, a system for measuring small deformation has been developed. The small strain measurement system (SSMS-II), which is improved from former system, is comprised of three components: the driving system, the instrumentation system, and control system.

The driving system consists of a stepper motor, a ball screw, and a ball spline. The stepper motor has a resolution of 1,228,800 steps per revolution. Its direction, step numbers, and speed can be controlled by users' program. The ball screw and ball spline are used for transforming rotational motion of stepper motor into a linear motion to generate cyclic or monotonic movement. Every 1 mm linear displacement needs 241,890 motor steps to achieve, the highly resolution is ideal for controlling a very small movement.

The instrumentation system includes electrical sensors and data acquisition device. A load cell is used to measure the tensile loadings. Two linear variable differential transducers (LVDT) are separately attached at the central part of geogrid to read its full range deformation. The variation of local strain is measured by two sets of non-contact proximitors. The effective measurement distance of proximitor is 0 to 2.0 mm. Its resolution is up to 12.5 nm (1.25×10^{-5} mm). Two proximitors are separately installed next to the LVDT. Figure 1 illustrates the schematic view of SSMS-II, Figure 2 shows the whole assembly system.

The control system controls the stepper motor and takes output readings. The direction, speed, and steps of stepper motor are assigned by a personal computer (PC) program to generate motion. A 22 bits analog/digital converter is used to transforms outputs to PC.

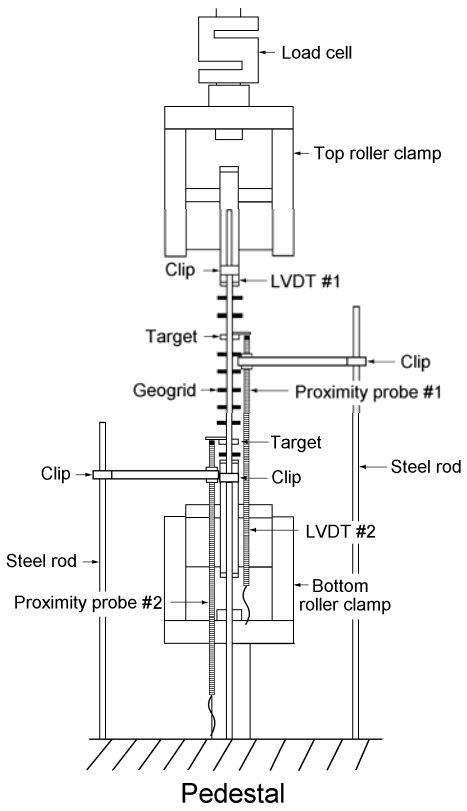

Figure 1. Schematic view of SSMS-II.

Figure 2. Equipment of SSMS-II.

3. RESULTS OF THE MONOTONIC TENSILE LOADING TESTS

For the sake of comparison, another tensile loading equipment (GT-AI-7000L) was used to carry out parts of tests. The capacity of load cell is 20,000 kgf. The deformation is measured by relative displacement of two steel wires which are clipped at the central of test material. Each wire connects to a roller counter at the top or bottom side of clamp. Figure 3 shows the equipment of GT-AI-7000L.

Figure 3. Equipment of GT-AI-7000L.

A series of monotonic tensile loading tests were performed to verify the capability of SSMS-II. The properties of tested geogrids are shown in Table 1. Two strain rates (Vs = 1%/min. and 10%/min.) were used and three strain levels (ε = 1%, 3%, and 4.5%) were measured by proximitors. Variables applied in this series of tensile loading tests are summarized in Table 2.

Table 1. Basic characteristics of tested geogrids.

Product name	Type	Polymer	Tensile strength (kN/m)
MD40	Woven geogrid with PVC coating	PET	51.54

Table 2. Variables applied in the tensile loading tests.

Test No.	Equipment	Strain rate (%/min.)	Sensors for measuring small strain	Strain level (%)
MD40-1 to MD40-5	SSMS-II	1	2 proximitors	1, 3, 4.5
MD40-6 to MD40-9	SSMS-II	10	none	-
GT-1 to GT-7	GT-AI-7000L	10	none	-

Figure 4 demonstrate the global load - strain curves under different Vs of SSMS-II. Figure 5 presents the global load - strain curves with Vs = 10 %/min. of GT-AI-7000L. Results show the repeatability for both of the equipments.

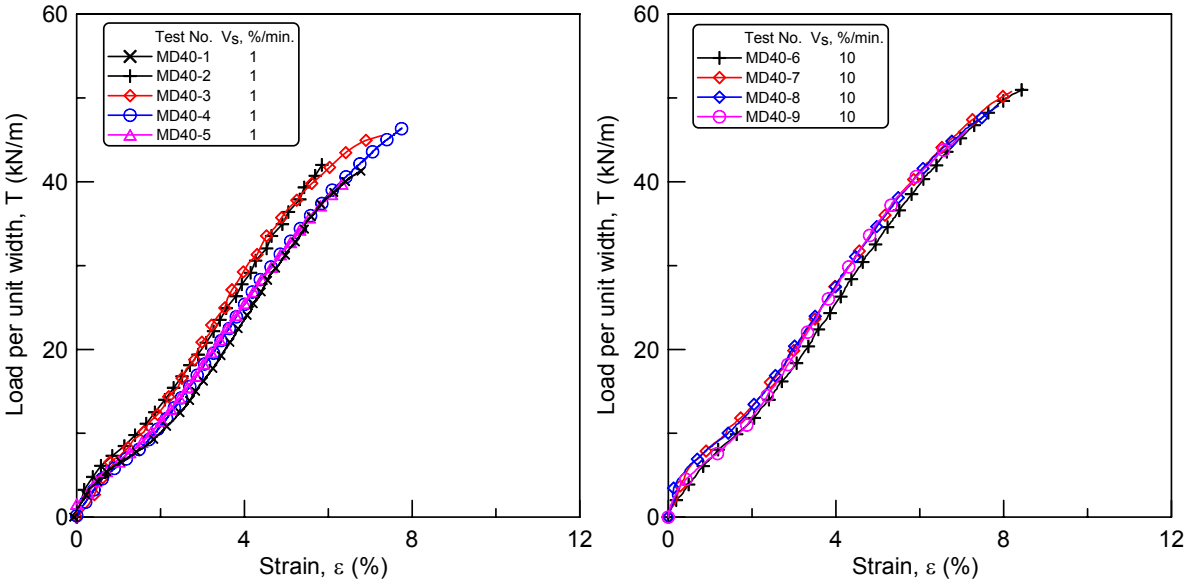

Figure 4. The global load - strain curves of SSMS-II.

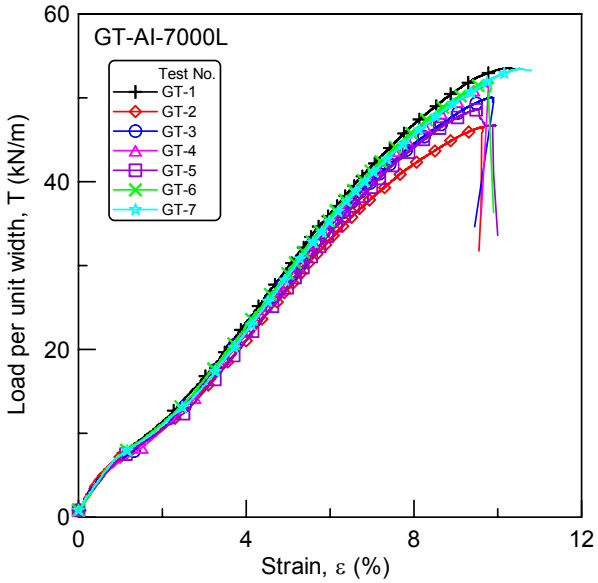

Figure 5. The global load - strain curves of GT-AI-7000L.

Two types of stiffness are proposed to illustrate the variation of global and local stiffness curves. As shown in Figure 6, the global secant stiffness (J_{sg}) is the slope of origin to the desired strain on the curve. The local secant stiffness (J_{sl}) is the slope of start point of a strain level to the desired strain on the curve.

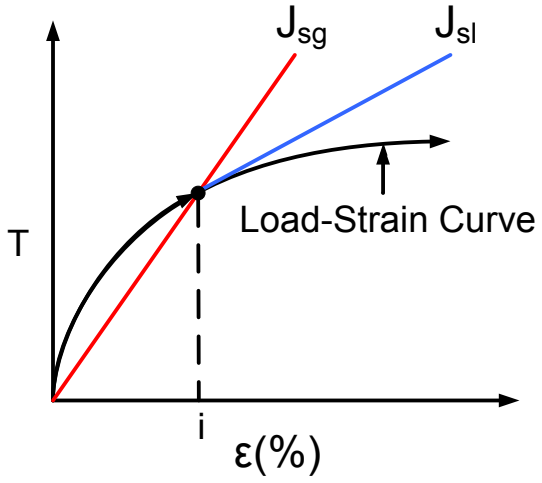

Figure 6. Definition of J_{sg} and J_{sl}.

Figures 7 to 9 demonstrate local load - strain curves at 3 strain levels (ε = 1%, 3%, and 4.5%). The measured local strains (ε_L) are within 0.3%, and curves obtained from readings of proximitors indicate a clear trend. According to the results of GT-AI-7000L, the load – strain curve becomes noisier at higher strain level. It implies that lots of PET yarns had been broken and/or slip occurs at fixed ends to cause the movement.

The J_{sl} is determined within ε_L = 0.3%, in such a small strain range it could be considered as a tangent stiffness. The J_{sl} curve represents the variation of stiffness at certain strain level, it can provide the WSA a more precise prediction.

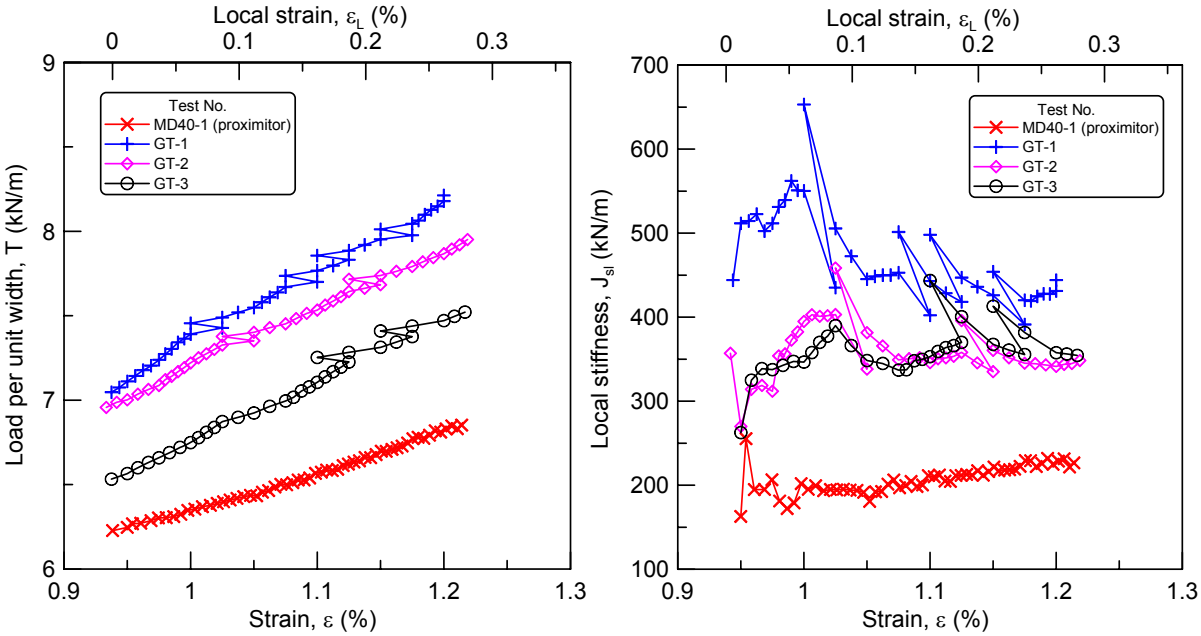

Figure 7. The local load - strain and J_{sl} - strain curves at strain level of 1%.

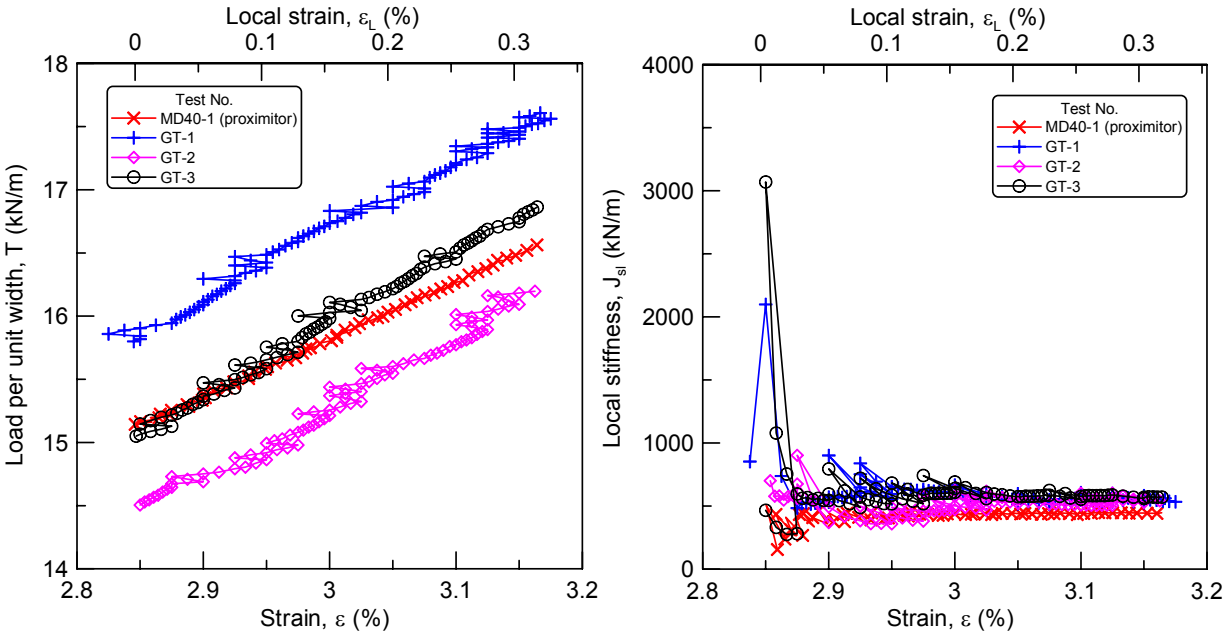

Figure 8. The local load - strain and J_{sl} - strain curves at strain level of 3%.

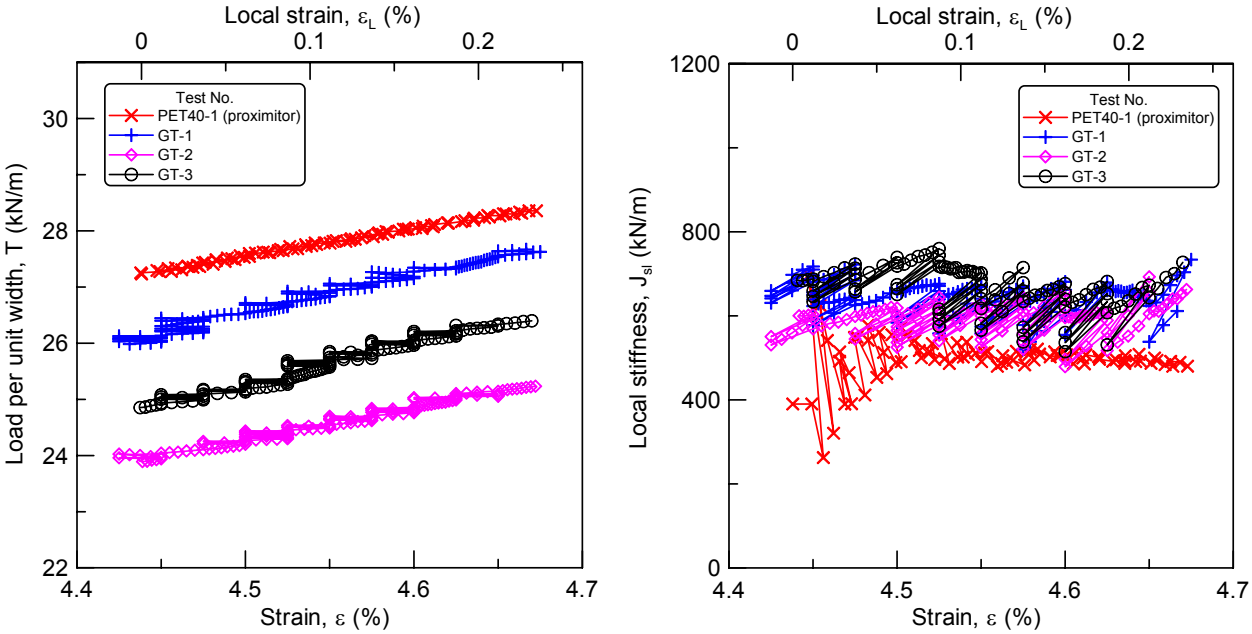

Figure 9. The local load - strain and J_{sl} - strain curves at strain level of 4.5%.

Figures 10 and 11 show the load – strain curve at different Vs, results indicate that the influence of Vs is not obvious. The J_{sg} - strain curves show SSMS-II can make a smoother curve than GT-AI-7000L.

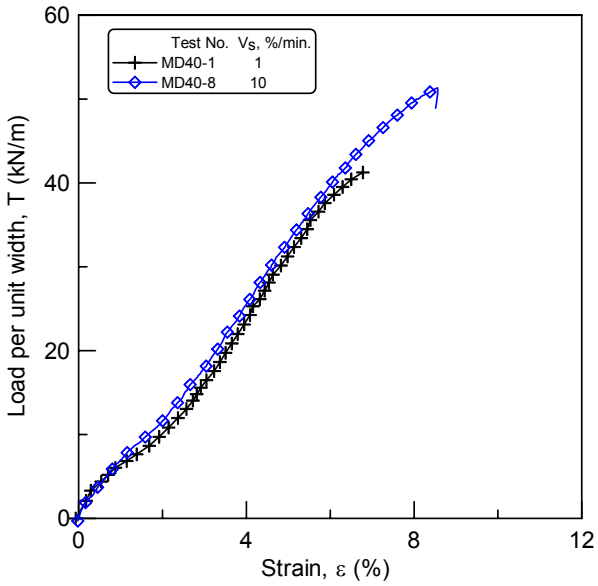

Figure 10. The global load - strain curves at different Vs.

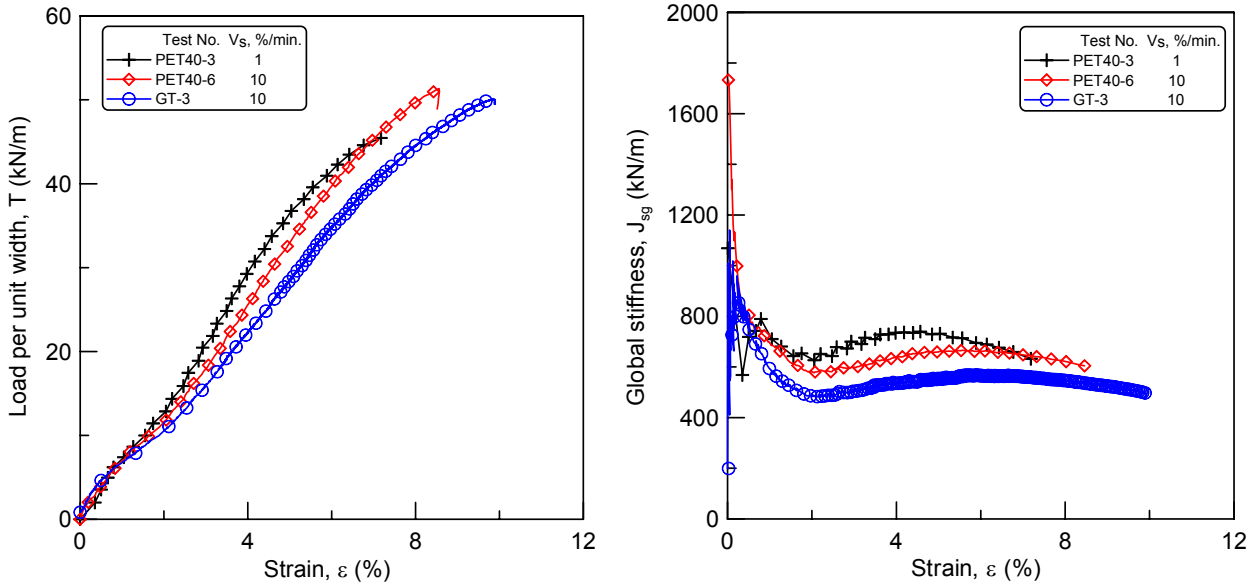

Figure 11. The global load - strain and J_{sg} - strain curves with different Vs and equipments.

4. CONCLUSIONS

A small strain measurement system (SSMS-II) has been developed and a series of tests have been performed to verify its capability. In the light of results, the conclusions are as follows:

(1) The step motor has high resolution makes it easier perform linear controlled tests. The Small Strain Measurement System (SSMS-II) is capable of performing monotonic and cyclic tensile tests. The stiffness under different strain levels can be reasonable established.

(2) Load - strain curves of PET MD40 under different strain rates (1%/min. and 10%/min.) show unobvious difference.

(3) The local load - strain curves (ε_L = 0 to 0.3%) at different strain levels (1, 3, and 4.5%) show the well performance of SSMS-II.

(4) In comparison of 3 strain levels, the local load - strain curve of GT-AI-7000L was noisier at higher strain level. There indicates lots of PET yarns had been broken and/or slip occurs at fixed ends to cause movement.

(5) The global stiffness (J_{sg}) represents the trend of global load - strain curve. Both of the GT-AI-7000L and SSMS-II can establish the J_{sg} - strain curves. However, the local stiffness (J_{sl}), which is similar to a tangent stiffness value, can actually present the variation of stiffness at certain strain level. While using WSA to get well predictions, the local stiffness variation curve at a designated strain level should be clearly established. In the light of test results, SSMS-II can achieve these requirements.

REFERENCES

Allen, T.M. and Bathurst, R.J. (2002). Soil reinforcement loads in geosynthetics walls at working stress conditions, *Geosynthetics International*, 9(5-6): 525-566.

Allen, T.M. and Bathurst, R.J. (2003). *Prediction of Reinforcement Loads in Reinforced Soil Walls*, Report No. WA-RD 522.2, Washington State Department of Transportation, Olympia, Washington, USA.

Atkinson, J.H. (2000). Non-linear soil stiffness in routine design, *Geotechnique*, 50(5): 487-508.

Atkinson, J.H. and Sallfors, G. (1991). Experimental determination of soil properties, *10th ECSMFE*, Florence, Italy, 3: 915-956.

Bathurst, R.J. and Cai, Z. (1994). In-isolation cyclic load-extension behavior of two geogrids, *Geosynthetics International*, 1(1): 1-19.

Bathurst, R.J., Allen, T.M. and Walters, D.L. (2002). Short-term strain and deformation behavior of geosynthetic walls at work stress conditions, *Geosynthetics International*, 9(5-6): 451-482

Walters, D.L., Allen, T.M. and Bathurst, R.J. (2002). Conversion of geosynthetic strain to load using reinforcement stiffness, *Geosynthetics International*, 9(5-6): 483-523.